



# Multifunctional Group Biomass in Biosorption of $\text{Cu}^{2+}$ from Aqueous Solution: Kinetics and Isotherm Studies

A. A. Inyinbor<sup>1\*</sup>, F. A. Adekola<sup>2</sup> and G. A. Olatunji<sup>2</sup>

<sup>1</sup>Department of Physical Sciences, Landmark University, P.M.B 1001, Omu Aran, Nigeria.

<sup>2</sup>Department of Industrial Chemistry, University of Ilorin, P.M.B 1515, Ilorin, Nigeria.

\*Corresponding Author Email: [inyinbor.adejumoke@landmarkuniversity.edu.ng](mailto:inyinbor.adejumoke@landmarkuniversity.edu.ng)

Received 22 May 2017, Revised 22 August 2017, Accepted 30 November 2017

---

## Abstract

A novel, fibrous and multifunctional group surface biosorbent was prepared from the waste of *Irvingia gabonensis* (Dika nut-DN) seed. The biosorbent potential in cheap environmental remediation was tested using aqueous copper solution as adsorbate. Percentage  $\text{Cu}^{2+}$  removal was as high as 70 %. Sorption data were tested with various isotherms and kinetics models. Monolayer sorption dominates the uptake of  $\text{Cu}^{2+}$  onto DN with maximum monolayer sorption capacity of 227.27 mg/g. Some level of multilayer sorption also occurred within the  $\text{Cu}^{2+}$ -DN system thus a greater than 0.9 correlation coefficient recorded for the Freundlich sorption isotherm. Possible  $\text{Cu}^{2+}$  uptake mechanism onto DN was proposed. Pseudo second order kinetics best described the biosorption data while desorption results showed that  $\text{Cu}^{2+}$  was stable on DN surface.

**Keywords:** Biomass, *Irvingia gabonensis*, Kinetics, Isotherms, Thermodynamics.

---

## Introduction

Heavy metals are common constituent of industrial wastewater. Industrial processes which utilize one or more heavy metals as catalysts or a part of their materials discharge wastewater with loads of heavy metals. Typical examples of such industry include the textile, electroplating, glass and ceramics, metal finishing and mining [1].

The discharge of heavy metals laden wastewater into the environment causes great deterioration and affects the aquatic organism as well as causes various health issues to human. For instance, exposure to copper may lead to various diseases such as, headache, respiratory problems, hepatic and renal damage, skin, gastrointestinal and central nervous system irritations, depression as well as necrotic changes in liver and kidney [2]. Therefore, effective wastewater treatment will suffice in attaining sustainable development and healthy living. Sorption of pollutants using activated carbon has been considered as a successful method of wastewater treatment. Its

operation that needs no expertise and its ability to deal with pollutants of very low concentrations makes this method attractive. Sorption however comes with the shortcoming of expensive activated carbon. Ability to find alternative to the expensive activated carbon will result in effective and affordable wastewater treatment and subsequently protect the environment.

Crop residue with various surface functional groups such as the hydroxyl, carbonyl, carboxylic, thiol, and amines amongst others have metal sequestering ability. These functional groups with heteroatom may remove metal ions via complex formation by donating their lone pair(s) of electron to the metals' empty d-orbital. Natural pores as well as fibers of crop residues are also greatly utilized during biosorption. Removal of various pollutants using various crop residue have been well reported [2, 3, 4, 5, 6, 7, 8, and 9].

The composition of various parts of a tree is usually similar. Cotyledon of *I. gabonensis* seed

is sufficiently rich in protein/amino acids thus have high Nitrogen, Oxygen, and Sulphur contents [10]. These atoms create sufficient binding sites for metal ions. The use of *I. gabonensis* waste in environmental remediation has not been well explored. Previously reported work in this regard was in the uptake of Rhodamine B dye [11]. Therefore, this work is focused on utilizing a novel bioadsorbent prepared from *I. gabonensis* waste biomass for the uptake of  $\text{Cu}^{2+}$  ions from aqueous solution. Detailed isotherm and kinetic analysis of sorption data were employed to establish the modes and mechanism of  $\text{Cu}^{2+}$  uptake. The spontaneous nature as well as reusability and stability of the biosorbent was also studied via thermodynamics and desorption analysis.

## Materials and methods

### *Biomass collection and preparation*

*I. gabonensis* endocarp waste (dika nut-DN) was collected from local farmers in Omu Aran, Kwara State, Nigeria. It was thoroughly washed with deionized water to remove dirt, dried in a low temperature oven overnight, grounded and screened into a particle size of 150-250 $\mu\text{m}$ . It was then stored in air tight container for further characterization and use.

### *Preparation of stock solution of $\text{Cu}^{2+}$*

A stock solution of 1000 mg/L of  $\text{Cu}^{2+}$  was prepared by dissolving 3.931 g of analytical grade  $\text{CuSO}_4 \cdot 5\text{H}_2\text{O}$  (Lobal Chemie, India) in 1 L of deionized water. Serial dilutions were done to obtain other desired lower concentrations.

### *Biosorbent Characterization*

The surface chemistry of biosorbent is of great importance in biosorption studies. Biomass, particularly agrowaste, which are lignocellulosic materials, have multi functional group surface. A FEI/SEM Quanta 200 for Scanning Electron Microscope (SEM) coupled with Energy dispersive X-ray (EDX) was employed for surface morphology and elemental composition analysis.

The Brunauer-Emmett-Teller (BET) surface area and the porosity of DN was determined using a Micromeritics Tristar II surface

area and porosity analyzer. Samples were degassed at 90 °C and temperature was subsequently increased to 200 °C overnight.

A Bruker Alpha Fourier Transform Infrared (FTIR) spectrometer was employed for the functional group determination. Samples were prepared by mixing dried DN and KBr (Merck, for spectroscopy) in a ratio 1 to 500 in an agate mortar, this mixture was then pressed at 10 tonnes  $\text{cm}^{-2}$  for 15 minutes under vacuum. The pH point of zero charge (pHpzc) was determined using our earlier reported method [11]

### *Biosorption theory and effects of operational parameters*

The uptake of metal ions by biomass largely depends on the available active biosorption sites on one side and the existence, mobility, amount of metal ion in solution and competing ions in solution on the other side.

### *Bioadsorbent loading effects*

In this study, effects of increased available active site on the biosorption of  $\text{Cu}^{2+}$  were investigated by varying the bioadsorbent dosage between 1 and 5 g/L. A given dose of the biosorbent was added to a 100 ml of 60 mg/L  $\text{Cu}^{2+}$  solution in a plastic bottle. In order to attain equilibrium, the mixture was agitated in a temperature controlled water bath shaker operated at 150 rpm and 26 °C for 120 minutes. The final mixture was separated by filtration and the residual metal ion was determined using an atomic absorption spectrophotometer (AAS, PerkinElmer AAnalyte 400).

### *Biosorption and pH effects*

Copper exists in various forms depending on the pH of the solution. At low pH,  $\text{Cu}^{2+}$  dominates and above the pH of 6.3 precipitation occurs as a result of hydroxyl Cu (II) formation [12]. Thus, the effects of pH on the biosorption of  $\text{Cu}^{2+}$  were carried out within the pH range of 1 and 6. The pH of the solution was adjusted using 0.1 M HCl or 0.1 M NaOH. A 0.1 g of the biosorbent was used for 100 mL of a 60 mg/L solution of  $\text{Cu}^{2+}$ .

The agitation time, temperature, agitation speed and residual metal ion determination are as afore described. The optimum pH was considered in subsequent biosorption studies.

#### ***Contact time and concentration effects on Cu<sup>2+</sup> uptake onto DN***

Biosorption may depend on the biosorbent reactive surface sites as well as the amount of adsorbate in solution [13]. Varying concentrations of adsorbate (20 mg/L, 40 mg/L, 60 mg/L, 80 mg/L and 100 mg/L) were used in this study. A 0.1 g of biosorbent was mixed with each concentration of adsorbate, which has been previously adjusted to its optimum pH in separate plastic bottles. The mixture was agitated in a temperature controlled water bath shaker operated at 26 °C and 150 rpm. Samples were withdrawn at intervals; the residual metal ion at each time was determined using an atomic absorption spectrophotometer (AAS, PerkinElmer AAnalyte 400) and this process continued until equilibrium was attained.

#### ***Biosorption and agitation speed effects***

The mobility of metal ion in solution may depend on the agitation speed and the temperature of the solution. Continuous bombardment of metal ion on biosorbent surface that is aided by agitation speed may facilitate biosorption process. In this study, agitation speed was varied between 150 and 300 rpm using the intervals of 50 rpm. A 100 ml of 60 mg/L Cu<sup>2+</sup> solution was used while the biosorbent dosage, agitation time, and temperature were maintained at 0.1 g, 120 minutes and 26 °C, respectively.

#### ***Biosorption and temperature effects***

The effects of temperature on biosorption of Cu<sup>2+</sup> onto DN were studied within the temperature range of 40 °C and 80 °C considering 10 °C intervals. A 100 mL of 60 mg/L Cu<sup>2+</sup> solution was used for the effects of temperature study. The biosorbent dosage, agitation time, and agitation speed were maintained at 0.1 g, 120 minutes, and 150 rpm respectively. The residual metal ion was determined as earlier described.

#### ***Biosorption and ionic strength effects***

Effluents generated from industries may not contain a single type of ion, thus the ionic strength of Cu<sup>2+</sup> solution was increased by the addition of NaCl solution of varying concentration (0.001, 0.01 and 0.1 M). A 100 mL of 60 mg/L Cu<sup>2+</sup> solution was used for this study. The bioadsorbent dosage, agitation time, agitation speed and temperature were maintained at 0.1 g, 120 minutes, 150 rpm and 26 °C, respectively. The residual metal ion was determined as earlier described.

#### ***Desorption experiments***

Regeneration of spent biosorbent provides information about the possible reusability of the biosorbent as well as uptake mechanism of pollutants. The affinity of Cu<sup>2+</sup> for biosorbent surface compared with organic, inorganic acid as well as water was tested. Thus, desorption studies were carried out using three different eluents (neutral water, 0.1 M HCl and 0.1 M CH<sub>3</sub>COOH). A 0.1 g of fresh biosorbent was added to 100 mL of 60 mg/L solution of Cu<sup>2+</sup> which had been previously adjusted to pH of 5 (optimum pH). The mixture was agitated using a temperature controlled water bath shaker operated at 26 °C and 150 rpm for 120 minutes. Loaded biosorbent was separated from the unbiosorbed metal ions (concentration of which was determined using AAS, PerkinElmer AAnalyst 400), it was washed gently with deionized water and subsequently dried. A 100 mL of each eluent was added to 0.1 g of loaded biosorbent, this mixture was agitated in a temperature controlled water bath shaker operated at 26 °C and 150 rpm for 120 minutes. The desorbed metal ion was determined using AAS, and desorption efficiency was calculated.

#### ***Mathematical analysis of biosorption data***

Percentage of metal ion removal, quantity of metal biosorbed at equilibrium, and desorption efficiency were calculated using mathematical relations 1, 2 and 3.

$$\% \text{ Removal} = \frac{(C_i - C_f)}{C_i} \times 100 \quad (1)$$

$$q_t = \frac{(C_i - C_f)XV}{M} \times 100 \quad (2)$$

$$\text{Desorption efficiency (\%)} = \frac{q_{de}}{q_{ad}} \times 100 \quad (3)$$

$C_i$ ,  $C_t$  and  $C_f$  are the adsorbate initial concentrations, adsorbate concentration at a given time  $t$  and adsorbate final concentration respectively.  $V$  is the volume of adsorbate used in liters and  $M$  is the mass of the biosorbent in g.  $q_{de}$  is the quantity desorbed by each of the eluent and  $q_{ad}$  is the adsorbed quantity during biosorbent loading.

### Mathematical modeling

Adsorbate uptake may be onto a uniform surface (monolayer biosorption), multiple surface (multilayer biosorption) while uptake of adsorbate may also occur via adsorbate-adsorbate interactions. Information concerning the mode of adsorbate uptake can be obtained via isotherms, kinetics, and mechanism models.

### Isothermal models

The Langmuir sorption isotherms [14] describes sorption onto a uniform surface, this is expressed by equation 4. The plot of  $C_e/q_e$  against  $C_e$  where  $C_e$  is the concentration of adsorbate in solution at equilibrium in mg/L and  $q_e$  is the quantity of adsorbate adsorbed at equilibrium in mg/g gives a straight line. Slope and intercept data is used to obtain the maximum monolayer sorption capacity ( $q_{max}$ ) and the Langmuir constant  $K_L$  in L/mg. Equation 4a expresses the dimensionless  $R_L$  factor which describe the favourability of the bioadsorption process.

The Freundlich isotherms [15] describes multilayer sorption and it is expressed by equation 5. The Freundlich constants  $K_f$  and  $n$  incorporates the factors affecting the adsorption capacity and adsorption intensity respectively. Temkin sorption isotherm [16] which assumes the linear decrease in heat of sorption while ignoring extreme concentrations. This may also justify adsorbate-adsorbate interactions in sorption processes. Temkin equation is expressed in equation 6 and Temkin constant ( $b$  in J/mol) related to the heat of

sorption can be obtained using equation 6a.  $A$  (L/g) and  $B$  are Temkin constants,  $T$  is temperature in kelvin while  $R$  is the gas constant (J/mol/K).

Dubinin-Radushkevich isotherm [17] expressed by equation 7 may explain whether adsorbate uptake was chemical or physical in nature. The Polanyi potential and the mean sorption energy can be obtained using equation 7 a and 7 b. The activity coefficient  $\beta$  is obtained from the slope of the plot of  $\ln q_e$  versus  $\epsilon^2$ .

$$\frac{C_e}{q_e} = \frac{C_e}{q_{max}} + \frac{1}{q_{max} K_L} \quad (4)$$

$$R_L = \frac{1}{(1 + K_L C_0)} \quad (4a)$$

$$\log q_e = \frac{1}{n} \log C_e + \log K_f \quad (5)$$

$$q_e = B \ln A + B \ln C_e \quad (6)$$

$$B = \frac{RT}{b} \quad (6a)$$

$$\ln q_e = \ln q_0 - \beta \epsilon^2 \quad (7)$$

$$\epsilon = RT \ln \left( 1 + \frac{1}{C_e} \right) \quad (7a)$$

$$E = \sqrt{\frac{1}{2\beta}} \quad (7b)$$

### Kinetics models

The pseudo first order model of Lagergren [18], pseudo second order kinetics model [19], Elovich [20] and Avrami [21] models were employed in the analysis of the kinetics data. The linear equations of these models are expressed as equation 8,9,10 and 11 respectively.

$$\ln[(q_e) - q_t] = \ln q_e - k_1 t \quad (8)$$

$$\frac{t}{q_t} = \frac{1}{k_2 q_e^2} + \frac{t}{q_e} \quad (9)$$

$$q_t = \frac{1}{\beta} \ln(\alpha\beta) + \frac{1}{\beta} \ln t \quad (10)$$

$$\ln[-\ln(1 - \alpha)] = n_{AV} K_{AV} + n_{AV} \ln t \quad (11)$$

$q_e$  and  $q_t$  are quantity adsorbed at equilibrium and at time  $t$  in mg/g.  $\alpha$  is a constant related to chemisorption rate and  $\beta$  is a constant which depicts the extent of surface coverage.  $K_{Av}$  is the Avrami constant and  $n_{Av}$  is the Avrami model exponent of time related to the change in mechanism of adsorption.  $k_1$  and  $k_2$  are the rate constant for the pseudo-first-order sorption  $\text{min}^{-1}$  and the rate constant of the pseudo-second-order kinetic  $\text{g/mg min}^{-1}$ .

### Mechanism models

The intraparticle diffusion model by Weber and Moris [22] and the Bangham models were further employed to ascertain biosorption mechanism. Equations 12 and 13 represent the linear form of these mechanism models.

$$q_t = k_{\text{diff}} t^{\frac{1}{2}} + C \quad (12)$$

$$\text{Log log} \frac{C_i}{(C_i - q_t M)} = \text{log} \frac{K_j M}{(2.303V)} + \alpha \text{log} t \quad (13)$$

$k_{\text{diff}}$  is the rate constant for intraparticle diffusion ( $\text{mg g}^{-1} \text{min}^{-1/2}$ ).  $C_i$  is the initial concentration of dye solution (mg/L),  $V$  is the volume of dye solution mL,  $M$  is the mass of the biosorbent (g/L),  $q_t$  is the quantity of dye sorbed at time  $t$  and  $\alpha$  ( $< 1$ ) and  $K_j$  are constants which can be obtained from the slope and intercept of Bangham plot respectively.

### Validation of kinetics model

The validity of the kinetics model was established using the chi square ( $X^2$ ) and normalized standard deviation ( $\Delta q_e$ ) represented by equations 14 and 15 respectively.

$$X^2 = \sum_{i=1}^n \frac{(q_{\text{exp}} - q_{\text{cal}})^2}{q_{\text{cal}}} \quad (14)$$

$$\Delta q_e (\%) = 100 \sqrt{\left[ \frac{(q_{\text{exp}} - q_{\text{cal}}) / q_{\text{exp}}}{N - 1} \right]} \quad (15)$$

### Thermodynamics study of biosorption of $\text{Cu}^{2+}$ onto DN

The randomness, spontaneity and feasibility of biosorption of  $\text{Cu}^{2+}$  onto DN was studied.

$$\ln K_o = \frac{\Delta S^\circ}{R} - \frac{\Delta H^\circ}{RT} \quad (16)$$

$$\Delta G^\circ = -RT \ln K_o \quad (17)$$

Where  $T$  is the temperature in Kelvin,  $R$  is the gas constant and  $K_o$  can be obtained from equilibrium concentration and quantity adsorbed at equilibrium. The values of enthalpy ( $\Delta H^\circ$ ) and  $\Delta S^\circ$  can be obtained from the plot of  $\ln K_o$  versus  $1/T$ .

## Results and Discussion

### Characteristics of biosorbent

Low BET surface was obtained for DN (Table 1); biosorbents may have several binding sites due to various surface functional groups they carry. These functional groups occupy pores and supposed available surfaces thus resulting into low surface areas of agro wastes [23]. The adventitious water in DN may have been responsible for its moderate affinity for water (% Moisture = 5.73) and high fixed carbon (71.42 %) characterized DN.

Table 1. Characteristics of biosorbent (DN).

Parameters	Values DN
pH	5.05
pHpzc	6.40
Bulk density ( $\text{g cm}^{-3}$ )	0.49
Moisture content (%)	5.73
Ash content (%)	3.46
BET surface area ( $\text{m}^2 \text{g}^{-1}$ )	0.0387
Average pore diameter (nm)	nd
%C	71.42
%O	28.36
%K	0.22

Porosity with vivid fibrous nature of agro wastes was depicted by the SEM micrograph of DN (Fig. 1a). However, after  $\text{Cu}^{2+}$  uptake swollen of DN fibers resulted (Fig. 1b).  $\text{Cu}^{2+}$  may have been absorbed into the pores thus the swollen fibers.

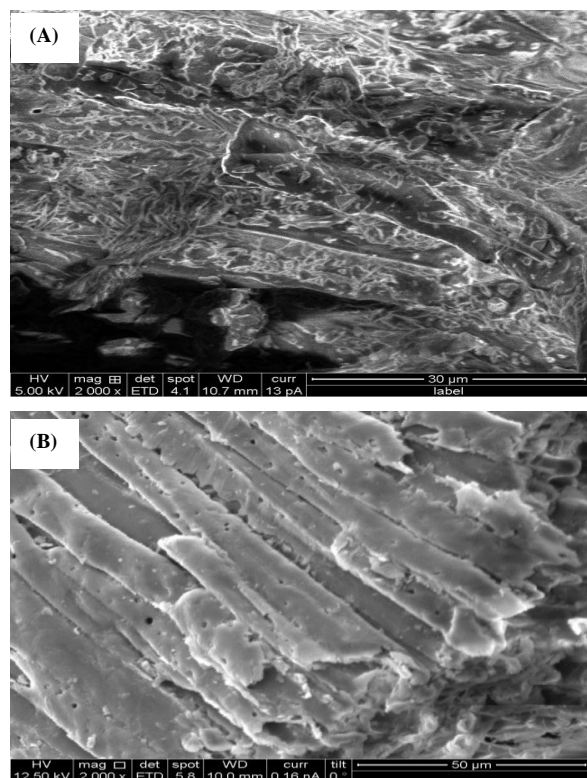


Figure 1. SEM of DN before  $\text{Cu}^{2+}$  adsorption (A) and after  $\text{Cu}^{2+}$  and sorption (B)

FTIR spectral of DN before and after  $\text{Cu}^{2+}$  uptake are shown in Fig. 2. DN showed characteristic absorption band of  $-\text{OH}$ ,  $-\text{C}-\text{H}$  and  $\text{C}-\text{OH}$  at  $3376\text{ cm}^{-1}$ ,  $2944\text{ cm}^{-1}$  and  $1033\text{ cm}^{-1}$  respectively.  $\text{C}=\text{O}$  vibration of carbonyl and methylene absorption bands were observed at  $1663\text{ cm}^{-1}$  and  $2932\text{ cm}^{-1}$ , respectively. The intensities of the observed absorption bands decreased after  $\text{Cu}^{2+}$  uptake (Fig. 2). Decrease in absorption bands intensity of the carbonyl and hydroxyl functional groups are more vivid. Possible DN- $\text{Cu}^{2+}$  surface reaction is presented in Scheme 1.

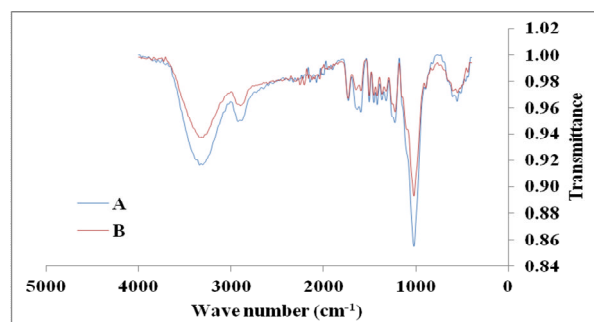
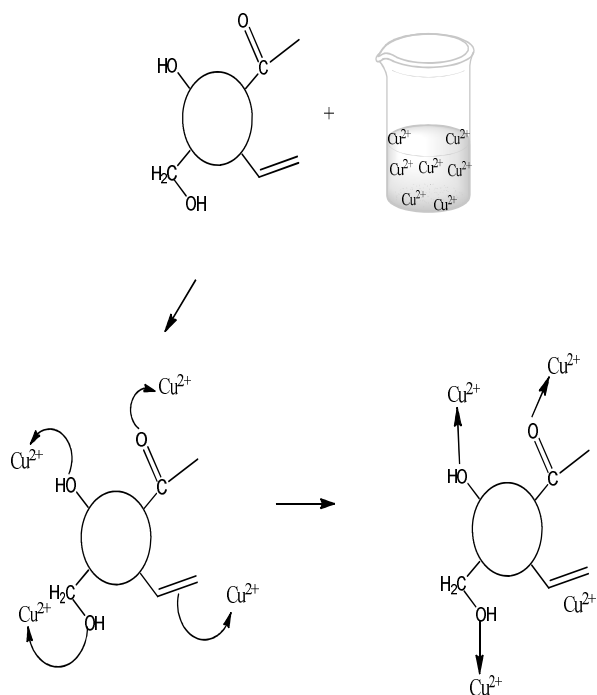


Figure 2. FTIR spectra of DN before  $\text{Cu}^{2+}$  uptake (A) and after  $\text{Cu}^{2+}$  uptake (B)



Scheme 1: Possible DN- $\text{Cu}^{2+}$  surface interactions

## $\text{Cu}^{2+}$ biosorption

### Biosorbent surface charge and adsorbate pH

Existence and behavior of adsorbate in solution as well as surface charge of the biosorbents greatly depends on the solution pH. The pH<sub>pzc</sub> of DN obtained was 6.40 (Table 1). At pH of 6.40, DN surface charge will be neutral while below 6.40 DN surface is positively charged. Hydroxonium ion is dominant in solution at low pH and copper ions exist as  $\text{Cu}^{2+}$  as well as  $\text{CuOH}^+$ , competition for sorption sites between copper ion and  $\text{H}_3\text{O}^+$  occur thus low uptake of  $\text{Cu}^{2+}$ . As adsorbate solution pH increases, the biosorbents surface becomes more negatively charged and deprotonation of functional groups occurs [24]. This creates more sites for  $\text{Cu}^{2+}$  uptake and subsequently increase in percentage  $\text{Cu}^{2+}$  removal was observed (Fig. 3).  $\text{Cu}^{2+}$  removal is highest at pH 5, above pH 5, precipitation of  $\text{Cu}(\text{OH})_2$  occurs hence inhibition of metal ions results.

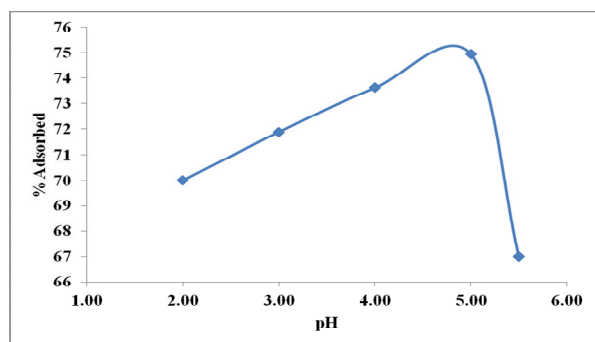


Figure 3. Effects of adsorbate solution pH on the biosorption of  $\text{Cu}^{2+}$  onto DN.

Conditions: Adsorbent dose (1 g/L), agitation speed (200 rpm), agitation time (120 minutes), Temperature (26 °C), Adsorbate concentration (60 mg/L).

#### Effects of adsorbent dosage on $\text{Cu}^{2+}$ uptake onto DN

Increase in biosorbent dosage creates more available surface sites thus increased uptake of  $\text{Cu}^{2+}$ . Percentage  $\text{Cu}^{2+}$  removal increased from 66.52 % at 1 g/L to 68.48 % at 4 g/L after which no further increase was observed in the  $\text{Cu}^{2+}$  removal (Fig. 4). Aggregation and overlap of biosorption sites may have resulted into the equilibrium attained after the 4 g/L dosage. The total amount of metal ion in solution did not increase, hence the decrease observed in quantity biosorbed per unit mass with increase in biosorbents dosage.

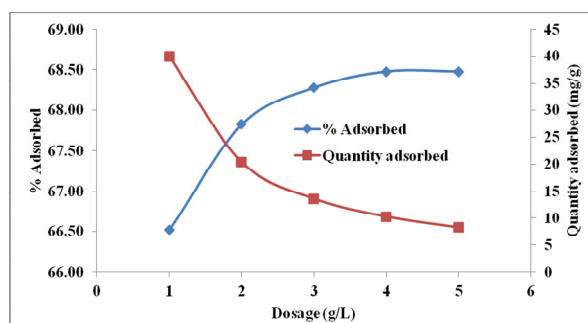


Figure 4. Effects of adsorbent dosage on the uptake of  $\text{Cu}^{2+}$  onto DN Conditions: Concentration 60 mg/L, agitation speed (200 rpm), agitation time (120 minutes), Temperature (26°C), pH 5.

#### Effects of agitation speed on $\text{Cu}^{2+}$ uptake onto DN

Rate of agitation increases biosorbent-adsorbate collision thus facilitating percolation of adsorbate into biosorbent pores. Slight increase in  $\text{Cu}^{2+}$  percentage removal was observed (about 0.97

% increase) as the agitation speed increased from 150 to 300 rpm (Fig. 5).  $\text{Cu}^{2+}$  uptake is mainly due to the functional groups. Since surface functional groups are readily exposed, agitation speed effect thus becomes negligible.

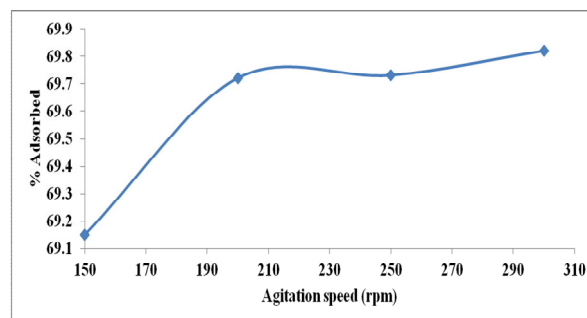


Figure 5. Effects of agitation speed on the uptake of  $\text{Cu}^{2+}$  onto DN Conditions: Concentration 60 mg/L, Dosage (1 g/L), agitation time (120 minutes), Temperature (26°C), pH 5.

#### Effects of ionic strength on $\text{Cu}^{2+}$ uptake onto DN

The quantity of  $\text{Cu}^{2+}$  adsorbed dropped drastically in the presence of electrolyte with about 50 % reduction. The decrease in  $\text{Cu}^{2+}$  uptake further decreased with increasing electrolyte concentration. Competition for adsorption site by  $\text{Na}^+$  and  $\text{Cu}^{2+}$  as well as mobility of  $\text{Cu}^{2+}$  may be responsible for the decrease in quantity of  $\text{Cu}^{2+}$  adsorbed in the presence of  $\text{Na}^+$  (Fig. 6). This effect was observed to decrease as the concentration of competing specie ( $\text{Na}^+$ ) decreased.

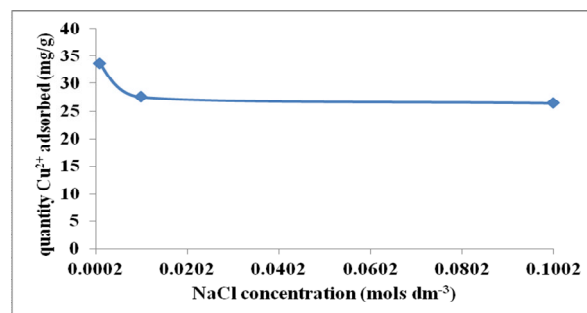


Figure 6. Effects of ionic strength on the uptake of  $\text{Cu}^{2+}$  onto DN Conditions: Concentration 60 mg/L, Dosage (1 g/L), agitation time (120 minutes), Agitation speed (200 rpm) pH 5, Temperature 27 °C.

#### Effect of initial concentration and contact time on $\text{Cu}^{2+}$ uptake onto DN

The uptake of  $\text{Cu}^{2+}$  onto DN was very rapid, between 94 % and 99 % of the total quantity

of  $\text{Cu}^{2+}$  was removed within the first 20 minutes. This may be because of interactions between exposed surface functional groups and  $\text{Cu}^{2+}$ . High initial concentrations provided driving force for adsorbate to overcome the mass transfer barrier between the aqueous and the solid interphase thus quantity adsorbed was found to increase as the initial concentration increased. Equilibrium was attained between 90 and 120 minutes across initial adsorbate concentrations considered. Continuous bombardment of copper ions with the biosorbent surface aids its percolation into the biosorbent pores thus  $\text{Cu}^{2+}$  uptake increased with time. Fig. 7 depicts the effects of contact time and concentration on  $\text{Cu}^{2+}$  uptake.

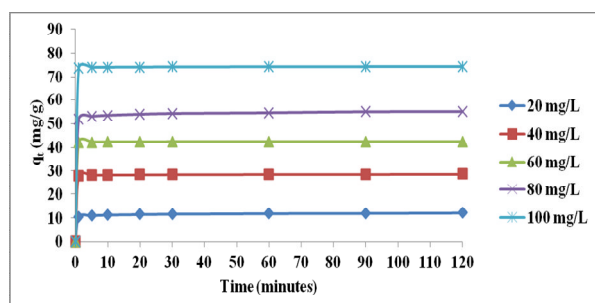


Figure 7. Effects of concentration/contact time on the uptake of  $\text{Cu}^{2+}$  onto DN

Conditions: Adsorbent dose (1g/L), agitation speed (200 rpm), agitation time (120 minutes), Temperature (26 °C), pH 5.

### Equilibrium data analysis

Based on the correlation coefficients, equilibrium adsorption data fitted best into the Langmuir adsorption isotherm suggesting that uptake onto a uniform surface dominates in this biosorption system. Percolation into biomass fibers and pores as well as adsorbate-adsorbate interactions may have also occurred thus the high Freundlich and Temkin correlation coefficient observed (Table 3). The favourability of the bioadsorption system was established by the dimensionless  $R_L$  value of less than unity (0.4366). Judging with the  $R^2$  values, equilibrium biosorption data fitted into the isotherms models in the order Langmuir>D-R>Freundlich>Temkin models. Energy of sorption obtained from the D-R model was 5.00 kJ/mol suggesting that the uptake of  $\text{Cu}^{2+}$  onto DN was physical in nature. The maximum monolayer sorption capacity obtained was 227.27 mg/g, this was compared with others

previously reported in literatures (Table 4), DN was observed to be highly efficient.

Table 3. Isotherm constants for the uptake of  $\text{Cu}^{2+}$  onto DN.

Isotherms	constants	DN
Langmuir	$q_{\max}$ (mg/g)	227.27
	$K_L$ (L.mg <sup>-1</sup> )	0.0129
	$R_L$	0.4366
	$R^2$	0.9813
Freundlich	$K_F$	0.9454
	n	0.7588
	$R^2$	0.9433
Temkin	A	6.063
	B	44.306
	b	56.29
	$R^2$	0.9159
D-R	$q_0$ (mg/g)	71.89
	$\beta$ (mol <sup>2</sup> .kJ <sup>-2</sup> )	0.02
	E(kJmol <sup>-1</sup> )	5.00
	$R^2$	0.9619

Table 4. Comparison of maximum monolayer biosorption capacity of  $\text{Cu}^{2+}$  onto DN with other previously reported works.

Adsorbents	$q_{\max}$ (mg/g)	References
Almond shell	9.00	[4]
Pine cone	4.60	[12]
Cashew nut shell	20.00	[25]
Peanut husk charcoal	0.35	[26]
Fly ash	0.18	[26]
Natural zeolite	1.12	[26]
Modified Moringa Oleifera	166.24	[27]
Pine cone shell	6.80	[28]
Loofah fiber	14.49	[29]
Coal dust	21.74	[30]
Tea waste	77.31	[31]
Dolomite	237.70	[31]
Tea waste and Dolomite	38.20	[31]
Acid treated water melon shell	27.03	[32]
Alkali treated water melon shell	31.25	[32]
Dika nut waste	227.27	This study

### Kinetics data analysis

Observing the close agreement in the calculated and experimentally determined quantity uptake at equilibrium ( $q_e$  calculated and  $q_e$  experimental), low values of  $X^2$  and  $\Delta q_e$  as well as high values of correlation coefficients (Table 5). The pseudo second order kinetics best described the DN- $\text{Cu}^{2+}$  biosorption system compared with other kinetics models. The Elovich modeling of DN- $\text{Cu}^{2+}$  biosorption data at various concentrations gave high correlation coefficient values ( $R^2 > 0.99$ ). The  $X^2$  and  $\Delta q_e$  are also characterized with low values. Elovich model is a good equation for sorption onto heterogeneous surface [33]. Correlation coefficients of various isotherms models were found to be high ( $R^2 > 0.9$  in all cases), suggesting

that while homogenous biosorption may have dominated the  $\text{Cu}^{2+}$  uptake onto DN, heterogeneous biosorption also reasonably occurred. Linear plot of the Bangham model suggests that while diffusion of adsorbate into the pore occurred, it was not the only mechanism of

adsorbate uptake onto DN. The Weber-Morris intraparticle diffusion plots (Figures not shown) did not pass through the origin, this suggests that intraparticle diffusion model was not the rate-limiting step. The boundary layer effect was also observed to increase with concentration.

**Table 5.** Pseudo-first-order, pseudo-second-order, Elovich, Avrami, intraparticle diffusion, and Bangham models parameters for the biosorption of  $\text{Cu}^{2+}$  onto DN.

Constants	Initial concentration				
	DN				
	20	40	60	80	100
$q_e$ experimental (mg/g)	12.18	28.70	42.43	55.02	74.33
<b>Pseudo first order</b>					
$q_e$ calculated (mg/g)	1.19	0.51	0.24	3.12	0.40
$K_1 \times 10^{-2}$ ( $\text{min}^{-1}$ )	2.36	2.17	3.31	4.88	3.89
$R^2$	0.9407	0.9172	0.9578	0.9083	0.9816
$\Delta q_e$ (%)	35.90	37.46	37.69	36.71	14.21
$X^2$	101.4959	1558.188	7416.65	863.3365	13664.11
<b>Pseudo second order</b>					
$q_e$ calculated (mg/g)	12.18	28.74	42.37	55.25	74.07
$K_2 \times 10^{-1}$ ( $\text{gmg}^{-1}\text{min}^{-1}$ )	1.02	2.42	6.19	0.59	3.65
$R^2$	0.9999	1.0000	1.0000	1.0000	1.0000
$\Delta q_e$ (%)	0.00	0.02	0.02	0.06	0.05
$X^2$	0.00	$5.57 \times 10^{-05}$	$8.5 \times 10^{-05}$	0.000957	0.000913
<b>Elovich</b>					
$\alpha_{E1}$ (mg/g.min)	$13.84 \times 10^{14}$	$4.87 \times 10^{82}$	$6.15 \times 10^{300}$	$1.53 \times 10^{34}$	$7.27 \times 10^{312}$
$\beta_{E1}$ (g/mg)	2.97	6.87	16.50	1.52	9.78
$R^2$	0.9986	0.9969	0.9979	0.9969	0.9964
$\Delta q_e$ (%)	1.89	0.01	0.00	0.02	0.004
$X^2$	$7.4 \times 10^{-5}$	$1.39 \times 10^{-5}$	0.00	$8.89 \times 10^{-5}$	$5.38 \times 10^{-6}$
<b>Avrami</b>					
$n_{Av}$	0.1672	0.1002	0.0989	0.1844	0.0878
$K_{Av}$ ( $\text{min}^{-1}$ )	3.97	12.62	15.61	5.03	17.99
$R^2$	0.9626	0.9579	0.8227	0.7546	0.8716
$\Delta q_e$ (%)	0.36	0.37	0.37	0.37	0.37
$X^2$	80.81	417.73	808.40	1564.26	2629.69
<b>Bangham</b>					
$\alpha \times 10^{-2}$	0.0296	0.0051	0.0014	0.0123	0.0014
$K_j \times 10^{-2}$ (g)	10.56	27.98	42.14	51.96	73.86
$R^2$	0.9980	0.9960	0.9970	0.9960	0.9960
<b>Intra particle diffusion</b>					
$C_1$ ( $\text{mgg}^{-1}$ )	10.729	28.065	42.175	52.333	73.916
$K_{diff}$ ( $\text{mgg}^{-1}\text{min}^{-1/2}$ )	0.1447	0.0626	0.0261	0.2806	0.0439
$R^2$	0.8946	0.8916	0.8944	0.8808	0.8897

### Effects of temperature and thermodynamics studies

Quantity of  $\text{Cu}^{2+}$  uptake was observed to decrease from 49.65 mg/g to 27.95 mg/g as temperature increased from 30 to 80 °C (Fig. 8). Breakdown of fibrous material vis-à-vis decrease in surface activities may have resulted to the decrease in the uptake of  $\text{Cu}^{2+}$  as the temperature

increased. Biosorption of  $\text{Cu}^{2+}$  onto DN was an exothermic process ( $\Delta H^\circ = -38.80$  kJ/mol) while a decrease in randomness at the solid-liquid interphase was observed during  $\text{Cu}^{2+}$  uptake onto DN ( $\Delta S^\circ = -111.10$  J/mol/K). Better interactions exist for  $\text{Cu}^{2+}$  and DN at ordinary room temperature thus negative  $\Delta G^\circ$  exists (Table 6). As  $\text{Cu}^{2+}$ -DN system temperature increased however,  $\text{Cu}^{2+}$  developed better affinity for water rather than

the biosorbents thus spontaneity/feasibility of  $\text{Cu}^{2+}$  uptake onto DN gradually decreased. At the highest system concentration, positive  $\Delta G^{\circ}$  was obtained.

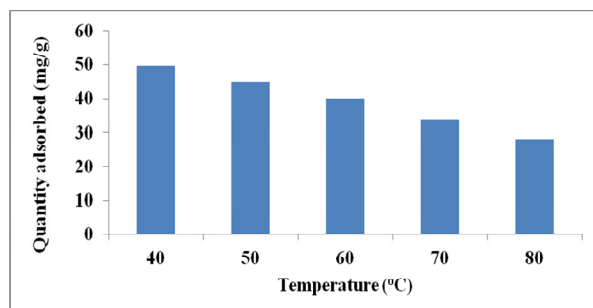


Figure 8. Effects of temperature on the uptake of  $\text{Cu}^{2+}$  onto DN  
Conditions: Concentration 60 mg/L, Dosage (1 g/L), agitation time (120 minutes), Agitation speed (200 rpm) pH 5.

Table 6. Thermodynamics parameters for biosorption of  $\text{Cu}^{2+}$  onto DN.

Adsorbent	$\Delta H^{\circ}$ (kJ/mol)	$\Delta S^{\circ}$ (J/ mol/K)	$\Delta G^{\circ}$ (kJ/mol)				
			313	323	333	343	353
DN	-38.80	-111.01	-4.08	-2.86	-1.92	-0.72	0.40

### Desorption studies

$\text{Cu}^{2+}$  was found to be stable on the surface of DN thus the desorption efficiencies were very low. The highest percentage desorption recorded was observed when acetic acid was used as eluent (Fig. 9). Although dika nut is abundantly available with its waste, which has no economic use and is continuously generated. However, appropriate desorbing eluent will further give DN more value.

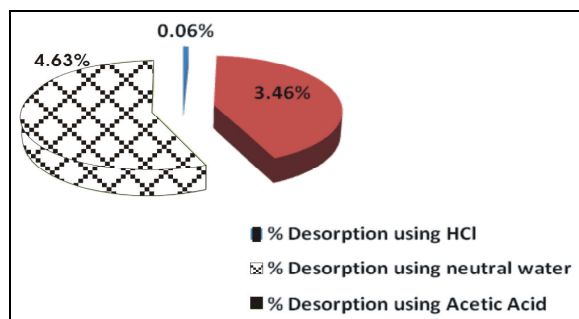


Figure 9. Percentage desorption for each of the eluents used for desorption

### Conclusion

The waste of *I. gabonensis* was found to be efficient in the removal of  $\text{Cu}^{2+}$  with some degree of heterogeneous sorption. Maximum monolayer sorption capacity was found to be high (272.27 mg/g). The surface area of DN was found to be low; this is the usual characteristics of agrowaste due to numerous surface functional groups. Surface functional group binding as well as pores and fibers penetration may be the modes of  $\text{Cu}^{2+}$  uptake; several binding sites available on DN surface may be responsible for  $\text{Cu}^{2+}$  stability on DN surface thus a low desorption is resulted. Possible interactions of  $\text{Cu}^{2+}$  with DN surface were proposed. Although Pseudo second order kinetics best described  $\text{Cu}^{2+}$  uptake onto DN, the Elovich model also effectively described the kinetics of the  $\text{Cu}^{2+}$ -DN system.

### References

- G. Huang, D. Wang, S. Ma, J. Chen, L. Jiang and P. Wang, *J. Colloid Interface Sci.*, 445 (2015) 294.  
<https://doi.org/10.1016/j.jcis.2014.12.099>
- G. Blázquez, M.A. Martín-Lara, E. Dionisio-Ruiz, G. Tenorio and M. Calero, *J. Ind. Eng. Chem.*, 17 (2011) 824.  
<https://doi.org/10.1016/j.jiec.2011.08.003>
- N. Gupta, A. K. Kushwaha and M. C. Chattopadhyaya, *J. Taiwan Inst. Chem. Eng.*, 43 (2012) 604.
- A. Ronda, M. A. Martín-Lara, E. Dionisio, G. Blázquez and M. Calero, *J. Taiwan Inst. Chem. Eng.*, 44 (2013) 466.  
<https://doi.org/10.1016/j.jtice.2012.12.019>
- Ş. Taşar, F. Kaya and A. Özer, Biosorption of lead (II) ions from aqueous solution by peanut shells, *J. Environm. Chem. Eng.*, 2 (2014) 1018.  
<https://doi.org/10.1016/j.jece.2014.03.015>
- S. Sadaf, H. N. Bhatti, S. Nausheen and M. Amin, *J. Taiwan Inst. Chem. Eng.*, 47 (2015) 160.  
<https://doi.org/10.1016/j.jtice.2014.10.001>
- F. Deniz and R. A. Kepekci, Dye biosorption onto pistachio by-product, *J. Mol. Liq.*, 219 (2016) 194.  
<https://doi.org/10.1016/j.molliq.2016.03.018>

8. S. Banerjee, G. C. Sharma, R. K. Gautam, M. C. Chattopadhyaya, S. N. Upadhyay and Y. C. Sharma, *J. Mol. Liq.*, 213 (2016) 162. <https://doi.org/10.1016/j.molliq.2015.11.011>
9. M. A. Martín-Lara, G. Blázquez, M. Calero, A.I. Almendros and A. Ronda, *Int. J. Miner. Process.*, 148 (2016) 72. <https://doi.org/10.1016/j.minpro.2016.01.017>
10. O. O. Ekpe, I. B. Umoh and O. U. Eka, *African J. Food, Agric. Nutr. Development* online, 7 (2007) 1. <file:///C:/Users/Imran%20Deswali/Downloads/136140-364634-1-SM.pdf>
11. A. A. Inyinbor, F. A. Adekola and G. A. Olatunji, *South African J. Chem.*, 68 (2015) 115. <https://doi.org/10.17159/0379-4350/2015/v68a17>
12. A. E. Ofomaja and E. B. Naidoo, *Chem. Eng. J.*, 175 (2011) 260. <https://doi.org/10.1016/j.cej.2011.09.103>
13. A. A. Inyinbor, F. A. Adekola and G. A. Olatunji, *Appl. Water Sci.*, (2016) 1. <DOI10.1007/s13201-016-0405-4>
14. I. Langmuir, *J. Am. Chem. Soc.*, 38 (1916) 2221. <https://doi.org/10.1021/ja02268a002>
15. H. M. F. Freundlich, *Z. Phys. Chem.*, 57 (1906) 385. <DOI: 10.4236/ajac.2013.47A001>
16. M. I. Temkin and V. Pyzhev, *Acta Physiochim. USSR*, 12 (1940) 327. <DOI: 10.4236/aces.2015.53037>
17. M. M. Dubinin and L. V. Radushkevich, *Proc. Acad. Sci. Phys. Chem. USSR*, 55 (1947) 331.
18. S. Lagergren and B. K. Svenska and R. Swed. *Acad. Sci. Doc, Band*, 24 (1898) 1.
19. Y. S. Ho and G. McKay, *Proc. Biochem.* 34 (1999) 451. [https://doi.org/10.1016/S0032-9592\(98\)00112-5](https://doi.org/10.1016/S0032-9592(98)00112-5)
20. C. Aharoni and M. Ungarish, *J. Chem. Soc. Farad. Trans.*, 72 (1976) 265.
21. M. Avrami, *J. Chem. Phys.*, 8 (1940) 212. <https://doi.org/10.1063/1.1750631>
22. W. J. Weber and J. C. Morris, *J. Sanitary Eng. Div. Am. Soc. Civil Eng.*, 89 (1963) 31.
23. A. A. Inyinbor, F. A. Adekola and G. A. Olatunji, *Water Resour. Industry*, 15 (2016) 14. <https://doi.org/10.1016/j.wri.2016.06.001>
24. A. S. Singha and A. Guleria, *Eng. Agric., Environm. Food*, (2014). <https://doi.org/10.1016/j.eaef.2014.08.001>
25. P. SenthilKumar, S. Ramalingam, V. Sathyaselvabala, S. Dinesh Kirupha and S. Sivanesan, *Desalination*, 266 (2011) 63. <https://doi.org/10.1016/j.desal.2010.08.003>
26. O. E. AbdelSalam, N. A. Reiad and M. M. ElShafei, *J. Adv. Res.*, 2 (2011) 297. <https://doi.org/10.1016/j.jare.2011.01.008>
27. H. K. Reddy, K. Seshaiyah, A. V. R. Reddy and S. M. Lee, *Carbohydr. Polym.*, 88 (2012) 1077. <https://doi.org/10.1016/j.carbpol.2012.01.073>
28. G. Blázquez, M. A. Martín-Lara, E. Dionisio-Ruiz, G. Tenorio and M. Calero, *J. Ind. Eng. Chem.*, 18 (2012) 1741. <https://doi.org/10.1016/j.jiec.2012.03.018>
29. X. Tang, Q. Zhang, Z. Liu, K. Pan, Y. Dong and Y. Li, *J. Mol. Liq.*, 191 (2014) 73. <https://doi.org/10.1016/j.molliq.2013.11.034>
30. M. Kapur and M. K. Mondal, *J. Taiwan Inst. Chem. Eng.*, 45 (2014) 1803. <https://doi.org/10.1016/j.jtice.2014.02.022>
31. A. B. Albadarin, J. Mo, Y. Glocheux, S. Allen, G. Walker and C. Mangwandi, *Chem. Eng. J.*, 255 (2014) 525. <https://doi.org/10.1016/j.cej.2014.06.029>
32. H. Gupta and P. R. Gogate, *Ultrason. Sonochem.*, 30 (2016) 113. <https://doi.org/10.1016/j.ultsonch.2015.11.016>
33. H. I. Inyang, A. Onwawoma and S. Bae, *Soil Tillage Res.*, 155 (2016) 124. <https://doi.org/10.1016/j.still.2015.07.013>